Published in final edited form as:
Cancer Res. 2016 December 01; 76(23): 6851–6863. doi:10.1158/0008-5472.CAN-16-1201.

Chemoresistance in Pancreatic Cancer Is Driven by Stroma-Derived Insulin-Like Growth Factors

Lucy Ireland[#1], **Almudena Santos**[#1], **Muhammad S. Ahmed**[1], **Carolyn Rainer**[1], **Sebastian R. Nielsen**[1], **Valeria Quaranta**[1], **Ulrike Weyer-Czernilofsky**[2], **Danielle D. Engle**[3,4], **Pedro A. Perez-Mancera**[1], **Sarah E. Coupland**[1], **Azzam Taktak**[5], **Thomas Bogenrieder**[6,7], **David A. Tuveson**[3,4,8], **Fiona Campbell**[1], **Michael C. Schmid**[1], and **Ainhoa Mielgo**[1]

[1]Department of Molecular and Clinical Cancer Medicine, University of Liverpool, Liverpool, United Kingdom

[2]Pharmacology and Translational Research, Boehringer Ingelheim RCV GmbH & Co KG, Vienna, Austria

[3]Cold Spring Harbor Laboratory, Cold Spring Harbor, New York

[4]Lustgarten Pancreatic Cancer Research Laboratory, Cold Spring Harbor, New York

[5]Department of Medical Physics and Clinical Engineering, Royal Liverpool University Hospital, Liverpool, United Kingdom

[6]Medicine and Translational Research, Boehringer Ingelheim RCV GmbH & Co KG, Vienna, Austria

[7]Department of Urology, University Hospital Grosshadern, Ludwig-Maximilians-University, Munich, Germany

[8]Rubenstein Center for Pancreatic Cancer Research, Memorial Sloan Kettering Cancer Center, New York, New York

[#] These authors contributed equally to this work.

Abstract

Corresponding Author: Ainhoa Mielgo, Department of Molecular & Clinical Cancer Medicine, Institute of Translational Medicine, University of Liverpool, Ashton street, First Floor Sherrington Building, Liverpool L69 3GE, United Kingdom. Phone: 44-01-5179-49555; amielgo@liverpool.ac.uk.

Disclosure of Potential Conflicts of Interest
T. Bogenrieder is a clinical program leader at Boehringer Ingelheim. No potential conflicts of interest were disclosed by the other authors.

Authors' Contributions
Conception and design: A. Mielgo
Development of methodology: L. Ireland, A. Santos, V. Quaranta, D.D. Engle, M.C. Schmid, A. Mielgo
Acquisition of data (provided animals, acquired and managed patients, provided facilities, etc.): L. Ireland, M.S. Ahmed, C. Rainer, S.R. Nielsen, V. Quaranta, U. Weyer-Czernilofsky, S.E. Coupland, D.A. Tuveson
Analysis and interpretation of data (e.g., statistical analysis, biostatistics, computational analysis): L. Ireland, M.S. Ahmed, S.E. Coupland, A.F. Taktak, T. Bogenrieder, F. Campbell, M.C. Schmid, A. Mielgo
Writing, review, and/or revision of the manuscript: U. Weyer-Czernilofsky, D.D. Engle, S.E. Coupland, A.F. Taktak, T. Bogenrieder, F. Campbell, A. Mielgo
Administrative, technical, or material support (i.e., reporting or organizing data, constructing databases): L. Ireland, V. Quaranta, D.D. Engle, P.A. Perez-Mancera, T. Bogenrieder, M.C. Schmid, A. Mielgo
Study supervision: A. Mielgo

Europe PMC Funders Author Manuscripts

Tumor-associated macrophages (TAM) and myofibroblasts are key drivers in cancer that are associated with drug resistance in many cancers, including pancreatic ductal adenocarcinoma (PDAC). However, our understanding of the molecular mechanisms by which TAM and fibroblasts contribute to chemoresistance is unclear. In this study, we found that TAM and myofibroblasts directly support chemoresistance of pancreatic cancer cells by secreting insulin-like growth factors (IGF) 1 and 2, which activate insulin/IGF receptors on pancreatic cancer cells. Immunohistochemical analysis of biopsies from patients with pancreatic cancer revealed that 72% of the patients expressed activated insulin/IGF receptors on tumor cells, and this positively correlates with increased $CD163^+$ TAM infiltration. *In vivo*, we found that TAM and myofibroblasts were the main sources of IGF production, and pharmacologic blockade of IGF sensitized pancreatic tumors to gemcitabine. These findings suggest that inhibition of IGF in combination with chemotherapy could benefit patients with PDAC, and that insulin/IGF1R activation may be used as a biomarker to identify patients for such therapeutic intervention.

Introduction

Drug resistance is one of the biggest challenges in cancer therapeutics and the cause of relapse in the majority of patients with cancer (1, 2). Therefore, understanding the molecular mechanisms by which cancer cells become resistant to therapies is critical to the development of durable treatment strategies. Mechanisms of resistance to therapies can be tumor cell intrinsic or mediated by the tumor microenvironment (3). We previously described intrinsic mechanisms of cancer cells' resistance to targeted therapy and radiotherapy (4–6). However, multiple factors can contribute to resistance to therapy and tumor progression, and one dominant player in solid cancers, and specifically in pancreatic cancer, is the presence of a rich protumoral microenvironment (7–10). In the pancreatic tumor microenvironment, macrophages and fibroblasts are the most abundant stromal cells, and engage in bidirectional interactions with cancer cells. Although tumor-associated macrophages (TAM) have the potential to kill cancer cells, we and others have shown that TAMs can promote tumor initiation, progression, metastasis, and also protect tumors from cytotoxic agents (11–23). Indeed, TAMs can be polarized into M1-like inflammatory macrophages that will activate an immune response against the tumor, or into M2-like immunosuppressive macrophages that promote tumor immunity and tumor progression (7, 24–26). Thus, therapeutics that can reprogram TAMs into M1-like macrophages or that specifically inhibit the protumoral functions of M2-like macrophages, rather than macrophage ablation therapies, may be more effective in the goal of restraining cancer progression (27, 28). However, the understanding of the precise molecular mechanisms by which TAMs and CAFs support tumor progression, and the use of combination therapies simultaneously targeting both protumoral stromal cells and cancer cells is only beginning to emerge.

Pancreatic ductal adenocarcinoma (PDAC) is a devastating disease, with one of the worst survival rates, and current standard therapies are unfortunately not very effective (29, 30). A characteristic feature of PDAC is an excessive tumor microenvironment with infiltrated immune cells that include macrophages (TAMs), and high numbers of activated fibroblasts, also known as myofibroblasts (31–33). In these studies, we sought to gain a better

Europe PMC Funders Author Manuscripts

understanding of the mechanism(s) by which TAMs and myofibroblasts support resistance of pancreatic cancer cells to chemotherapy with the aim to find innovative treatment combinations using conventional cytotoxic agents with therapies targeting the protumorigenic functions of stromal cells.

Materials and Methods

Generation of primary KPC-derived pancreatic cancer cells

The murine pancreatic cancer cells KPC FC1242 were generated in the Tuveson lab (Cold Spring Harbor Laboratory) isolated from PDAC tumor tissues obtained from LSL-Kras^{G12D}; LSL-Trp53^{R172H}; Pdx1-Cre mice of a pure C57BL/6 background as described previously with minor modifications (34). KPC cells were isolated in our laboratory from PDAC tumor tissues obtained from LSL-Kras^{G12D}; LSL-Trp53^{R172H}; Pdx1-Cre mice in the mixed 129/SvJae/C57Bl/6 background as described previously (for more details, see Supplementary Data; ref. 35).

Cell lines

SUIT-2 and MIA-PaCa-2 human pancreatic cancer cell lines were cultured in DMEM supplemented with 10% FBS, 1% penicillin/streptomycin, at 37°C, 5% CO_2 incubator. SUIT-2 cells were obtained in 2012 and MIA-PaCa-2 cells in 2010, and both were last authenticated by Eurofins in June 2016, and periodically tested and resulted negative for mycoplasma contamination.

Generation of primary macrophages, primary pancreatic myofibroblasts, macrophage, and myofibroblasts conditioned media

Primary murine macrophages were generated by flushing the bone marrow from the femur and tibia of C57BL/6 or mixed 129/SvJae/C57Bl/6 (PC) mice followed by incubation for 5 days in DMEM containing 10% FBS and 10 ng/mL murine M-CSF (PeproTech). Primary human macrophages were generated by purifying $CD14^+$ monocytes from blood samples obtained from healthy subjects using magnetic bead affinity chromatography according to manufacturer's directions (Miltenyi Biotec) followed by incubation for 5 days in DMEM containing 10% FBS and 50 ng/mL recombinant human M-CSF (PeproTech). Primary pancreatic stellate cells were isolated from C57BL/6 mice pancreas by density gradient centrifugation, and were activated into myofibroblasts by culturing them on uncoated plastic dishes in Iscove's Modified Dulbecco's Medium with 10% FBS.

To generate macrophage (MCM) and myofibroblasts conditioned media (MyoCM), cells were cultured in serum-free media for 24 to 36 hours, supernatant was harvested, filtered with 0.45-μm filter, concentrated using StrataClean Resin (Agilent Technologies), and immunoblotted for insulin-like growth factors (IGF) 1 and IGF2 (Abcam), or stored at −20°C.

Treatment with chemotherapy, MCM, blocking antibodies, and recombinant IGF

SUIT-2, MIA-PaCa-2, and KPC-derived cells were cultured in DMEM with 2% FBS for 24 hours, pretreated for 3 hours with MCM, or MyoCM, recombinant IGF (PeproTech 100-11)

at 100 ng/mL, or IGF-blocking antibody (Abcam 9572) at 10 μg/mL followed by gemcitabine (Sigma G2463) at 200 nmol/L, nabpaclitaxel 10, 100, or 1,000 nmol/L, paclitaxel (Sigma T7402) at 200 nmol/L or 5-FU (Sigma F6627) at 100 μmol/L. Cells were harvested after 24 to 36 hours and analyzed for Annexin-V/PI staining by flow cytometry.

RTK arrays and immunoblotting

Cells were serum starved or treated with MCM for 30 minutes or 3 hours, harvested, and lysed in RIPA buffer (150 mmol/L NaCl, 10 mmol/L Tris-HCl pH 7.2, 0.1% SDS, 1% Triton X-100, 5 mmol/L EDTA) supplemented with a complete protease inhibitor mixture (Sigma), a phosphatase inhibitor cocktail (Invitrogen), 1 mmol/L phenylmethylsufonylfluoride and 0.2 mmol/L Na_3VO_4. Cell lysates were analyzed with the Phospho-RTK Array Kit (R&D Systems). Immunoblotting analyses were performed using antibodies listed in Supplementary Data.

Syngeneic orthotopic pancreatic cancer models

Two orthotopic syngeneic pancreatic cancer models and two IGF-blocking antibodies were used in these studies. In one model, 1×10^6 primary $KPC^{luc/zsGreen}$ (zsGreen) cells ($FC1242^{luc/zsGreen}$) isolated from a pure C57Bl/6 background were implanted into the pancreas of immunocompetent syngeneic C57Bl/6 six- to 8-week-old female mice, and tumors were established for one week before beginning treatment. Mice were administered intraperitoneally with gemcitabine (100 mg/kg), IGF-blocking antibody BI 836845 (100 mg/kg; ref. 36) kindly provided by Boehringer Ingelheim, or IgG isotype control antibody, every 2–3 days for 10–15 days before harvest. The second model is described in Supplementary Data.

Gene expression

Total RNA was isolated from purified cells as described for Qiagen RNeasy protocol. Total RNA from entire pancreatic tumor tissues was extracted using a high salt lysis buffer (guanidine thiocynate 5 mol/L, sodium citrate 2.5 μmol/L, lauryl sarcosine 0.5% in H_2O) to improve RNA quality followed by purification using Qiagen RNeasy protocol. cDNA was prepared from 1 μg RNA per sample, and qPCR was performed using gene-specific QuantiTect Primer Assay primers from Qiagen. Relative expression levels were normalized to *gapdh* expression according to the formula $<2^{-(C_{t\text{gene of interest}} - C_{t\text{gapdh}})}$ (37).

Analysis and quantification of immune cells in pancreatic tumors by flow cytometry

Single-cell suspensions from murine pancreatic tumors were prepared by mechanical and enzymatic disruption in Hank's Balanced Salt Solution with 1 mg/mL Collagenase P (Roche; for more details, see Supplementary Data).

Immunohistochemical analysis

Deparaffinization and antigen retrieval was performed using an automated DAKO PT-link. Paraffin-embedded human and mouse PDAC tumors were immunostained using the DAKO envision+ system-HRP. Tissue sections were incubated for 1 hour at room temperature with primary antibodies described in Supplementary Data.

Immunofluorescence

Human and mouse PDAC frozen tissue sections were fixed with cold acetone, permeabilized in 0.1% Triton, blocked in 8% goat serum, and incubated overnight at 4°C with anti-phospho insulin/IGFR (R&D Systems), CD68 (DAKO, clone KP1), CK19 (Abcam), CK11 (Cell Signaling Technology), αSMA (Abcam), and EpCAM (BD Pharmingen).

Results

Macrophage-derived IGFs activate insulin and IGF1 receptors signaling in pancreatic cancer cells and induce chemoresistance

We and others have previously shown that inhibition of myeloid cell infiltration into tumors restrains cancer progression and increases response to chemotherapy (12, 14, 15, 18–22).

To gain a better understanding of the molecular mechanisms by which macrophages modulate pancreatic cancer cells' response to chemotherapy, we cultured human and mouse pancreatic cancer cells with MCM from primary human and mouse macrophages in the presence or absence of the standard chemotherapeutic agent gemcitabine. Primary human and mouse macrophages were generated using macrophage colony stimulating factor 1 (M-CSF1), which favors an M2-like phenotype (38), which was further confirmed by high expression of CD206 (M2 macrophage marker) and lack of IL12 (M1 macrophage marker; Supplementary Fig. S1A and S1B). We found, that MCM can directly induce chemoresistance of human and mouse pancreatic cancer cells to gemcitabine (Fig. 1A). Mechanistically, a phospho-receptor tyrosine kinase array of pancreatic cancer cells cultured in the presence or absence of MCM revealed that MCM induces the phosphorylation and activation of three receptor tyrosine kinases (RTK), insulin receptor (number 1), AXL receptor (number 2) and Ephrin receptor (number 3) (Fig. 1B). Insulin/IGF1 receptor signaling is known to be involved in drug resistance in various cancers (39). However, a direct role for macrophages in chemoresistance of pancreatic cancer via macrophage-dependent activation of the Insulin and IGF1 receptors has so far never been described. Thus, in this report, we further focused on investigating the role of insulin/IGF1 receptor activation by macrophages in pancreatic cancer chemoresistance. Activation of insulin and IGF1 receptors by macrophages was further confirmed by immunoblotting analysis (Fig. 1C) and by detection of tyrosine phosphorylation on insulin and IGF1 receptors immunoprecipitated from SUIT-2 human pancreatic cancer cells cultured in the presence or absence of MCM (Fig. 1D). Insulin and IGF1 receptors can bind three ligands: insulin, IGF-1, and IGF-2 (40). We found that primary human and mouse macrophages express mRNA levels of *Igf-1* and *Igf-2* but not *Insulin* (Fig. 1E and F and Supplementary Fig. S1C and S1D). We also found IGF1 and IGF2 proteins in primary human and mouse MCM and macrophage lysates (Fig. 1G). However, we could hardly detect any expression of IGFs nor insulin in pancreatic cancer cells (Supplementary Fig. S1E). Thus, these findings suggest that activation of insulin and IGF1 receptors on pancreatic cancer cells is triggered through paracrine macrophage-derived IGF1/IGF2 signaling. Interestingly, alternatively (IL4) activated M2 macrophages expressed higher levels of IGFs compared with classically (IFNγ/LPS) activated M1 macrophages (Supplementary Fig. S1C and S1D). Immunoblotting analysis of SUIT-2 human pancreatic cancer cells and KPC-derived murine

pancreatic cancer cells stimulated with MCM revealed that MCM activates insulin/IGF1R signaling to a similar degree as recombinant IGF (Fig. 1H). Importantly, blockade of IGF ligands with an IGF-neutralizing antibody was able to prevent macrophage-dependent activation of insulin/IGF1 receptors and the downstream effectors IRS1, IRS2, and AKT (Fig. 2A), and to inhibit macrophage-induced chemoresistance of human and mouse pancreatic cancer cells to gemcitabine (Fig. 2B–D). In addition, recombinant IGF was sufficient to mediate resistance of pancreatic cancer cells to chemotherapy, in a similar way to MCM (Fig. 2C– F). In the absence of chemotherapy, treatment of tumor cells with MCM, IGF-blocking antibody, or recombinant IGF alone did not alter the survival or proliferation of cancer cells (Supplementary Fig. S2A and S2B). *In vitro* exposure of pancreatic cancer cells to MCM was also able to enhance resistance of cancer cells to paclitaxel and 5-fluorouracil (5-FU) (Supplementary Fig. S3A– S3C). These findings suggest an important role for macrophage-derived IGFs in activating the insulin/IGF1 receptor survival signaling pathway in pancreatic cancer cells, and in enhancing resistance to chemotherapy.

Insulin and IGF receptors are activated on tumor cells in biopsies from pancreatic cancer patients, and this positively correlates with increased TAMs

We next evaluated whether the insulin/IGF1 receptor signaling is activated in biopsies from patients with pancreatic cancer, and whether this correlates with increased macrophage infiltration. Immunofluorescent and immunohistochemical staining of phospho-insulin and phospho-IGF1 receptors in biopsies from patients with PDAC revealed that insulin/IGF1R signaling is activated in pancreatic cancer cells in 38 of 53 (~72%) consented patients (Fig. 3A–C and Supplementary Fig. S4A and S4B; Supplementary Tables S1 and S2). Similarly, immunofluorescent and immunohistochemical staining of CD68 (pan-myeloid/macrophage marker) and CD163 (macrophage marker, commonly used to identify M2-like macrophages in human tissues) in the same frozen and paraffinembedded human PDAC samples showed that pancreatic tumors are infiltrated by $CD68^+$ and $CD163^+$ macrophages, which surround the phospho-insulin/$IGF1R^+$ ductal epithelial pancreatic cancer cells (Fig. 3D and Supplementary Fig. S4C and S4D). As we observed that M2-like macrophages express IGF ligands (Fig. 1E–G and Supplementary Fig. S1C and S1D), we subsequently analyzed, by IHC, serial sections from patients with PDAC for the copresence of $CD163^+$ (M2-like) macrophages and phospho-insulin/$IGF1R^+$ tumor cells. Importantly, we found that activation of insulin/IGF1 receptors positively correlates with increased infiltration of $CD163^+$ (M2-like) macrophages (Fig. 3E and F; Supplementary Tables S1 and S2). Immunofluorescent costaining of TAMs and IGFs confirmed that, in PDAC patient samples, TAMs express both IGF1 and IGF2 (Fig. 3G).

TAMs and myofibroblasts are the main sources of IGFs in the pancreatic tumor microenvironment

To determine whether TAMs are the main source of IGFs within the pancreatic tumor microenvironment, we orthotopically implanted murine primary pancreatic cancer cells derived from the genetically engineered mouse model of pancreatic cancer (LSL-$Kras^{G12D}$; LSL-$Trp53^{R172H}$; Pdx1-Cre mice; KPC) into syngeneic immunocompetent recipient mice. Hematoxylin and eosin (H&E), immunohistochemical, and immunofluorescent stainings with CD68, CD206, and αSMA, and flow cytometry analysis of these tumors, showed that

these mice developed PDAC, and that similar to human PDAC, these tumors are infiltrated by immune cells, including macrophages (Fig. 4A and B and Supplementary Fig. S5A), and are rich in αSMA$^+$ myofibroblasts (Supplementary Fig. S5A and S5B; refs. 32, 41–43). Importantly, murine PDAC orthotopic tumors also showed phosphorylation of insulin/IGF1R on tumor cells (Fig. 4A). In addition, similar to the orthotopically implanted PDAC tumors, spontaneous PDAC tumors derived from the genetically engineered KPC model also showed activation of insulin/IGF1R on tumor cells surrounded by CD206$^+$ TAMs and αSMA$^+$ myofibroblasts (Supplementary Fig. S6).

To determine whether *in vivo,* pancreatic TAMs are the main source of IGFs, we isolated TAMs (F4/80$^+$ cells) from established orthotopic PDAC tumors and assessed the expression levels of *Igf-1* and *Igf-2*. In agreement with our previous findings (Figs. 1E and F and 3G), we found that intratumoral macrophages isolated from murine pancreatic tumors express higher levels of *Igf-1* and *Igf-2* compared with F4/80$^-$ cells (Fig. 4C).

To further investigate this, we used a second KPC-derived cell line (FC1242) stably labeled with zsGreen reporter gene. As previously described, KPC-derived zsGreen cells were orthotopically implanted into the pancreas of syngeneic recipient mice (Fig. 4D). Tumors were harvested at day 23, and tumor cells (CD45$^-$/zsGreen$^+$), nonimmune stromal cells (CD45$^-$/zsGreen$^-$), M1-like macrophages (CD45$^+$/F4/80$^+$/CD206$^-$) and M2-like macrophages (CD45$^+$/F4/80$^+$/CD206$^+$) were sorted by flow cytometry (Supplementary Fig. S7A) and analyzed for the expression of *Igf-1* and *Igf-2*. This model further confirmed that orthotopic pancreatic tumors are infiltrated by both CD206$^+$ (M2-like) and CD206$^-$ (M1-like) TAMs (Fig. 4E) and revealed that both CD206$^+$ (M2-like macrophages) and αSMA$^+$ stromal cells, also known as myofibroblasts, are the main sources of IGFs in pancreatic tumors (Fig. 4F and Supplementary Fig. S7B). The ability of pancreatic myofibroblasts to produce IGFs was further assessed *ex vivo* in myofibroblasts and MyoCM (Supplementary Fig. S8A–S8C), as well as their capacity to enhance the resistance of tumor cells to chemotherapy (Supplementary Fig. S8D). Similarly, Tape and colleagues, recently found, using a proteomic approach, that *in vitro*, fibroblasts exposed to KPC-derived cells produce IGF, which promotes proliferation and survival of pancreatic cancer cells (44). In agreement with these findings, we also found high levels of IGF1 and IGF2 proteins in areas that are rich in macrophages and myofibroblasts in biopsies from patients with PDAC (Supplementary Fig. S9).

Blockade of IGFs improves response to gemcitabine in a preclinical tumor model of pancreatic cancer

Macrophages and myofibroblasts are the most abundant non-malignant stromal cells within the tumor microenvironment in PDAC (33). As we found that TAMs and myofibroblasts express IGFs in the pancreatic tumor microenvironment and stromal-derived IGFs enhance the resistance of pancreatic cancer cells to chemotherapy *in vitro*, we hypothesize that inhibition of IGFs could increase pancreatic cancer response to chemotherapy *in vivo*.

To test this hypothesis, we treated mice bearing established orthotopic pancreatic tumors with control IgG antibody, gemcitabine alone, IGF-blocking antibody (BI 836845) alone, or gemcitabine combined with BI 836845 (Fig. 5A). As previously shown (22, 32, 41, 43), and

similar to what is observed in patients with PDAC, gemcitabine alone had little or no effect on tumor growth in this model (Fig. 5B). Treatment with BI 836845 IGF-blocking antibody alone, only showed a modest effect on tumor growth. In contrast, combination of gemcitabine with BI 836845 significantly reduced tumor growth (Fig. 5B). Analysis of immune cell populations within the different treatment groups showed an increase in $F4/80^+$ macrophages in gemcitabine and gemcitabine+ BI 836845–treated tumors (Fig. 5C and Supplementary Fig. S10); however, the ratio of $CD206^-$ (M1-like) and $CD206^+$ (M2-like) macrophages within tumors remained the same in all treatment groups (Fig. 5D). In addition, the percentage of inflammatory monocytes ($Ly6C^+Ly6G^-CD11b^+F4/80^-$), neutrophils/myeloid-derived suppressor cells ($Gr1^+$ $CD11b^+F4/80^-$), and cytotoxic $CD8^+$ T lymphocytes ($CD3^+CD8^+$; CTL) remained similar in all treatment groups (Fig. 5C). Immunohistochemical analysis of tumors showed that phosphorylation of insulin and IGF1 receptors was decreased in tumors treated with BI 836845 IGF-blocking antibody (Fig. 5E and Supplementary Fig. S11). Importantly, immunohistochemical staining of cleaved caspase-3 revealed significantly higher levels of cell death in tumors treated with the combination of gemcitabine and BI 836845, compared with control, gemcitabine alone, or BI 836845 alone groups (Fig. 5E and F).

To confirm these results, we repeated a similar experiment using a second KPC-derived cell line, and a commercially available IGF-blocking antibody from Abcam (ab9572). This second *in vivo* experiment yielded very similar results, and showed a significant decrease in tumor growth in mice treated with the combination of gemcitabine/IGF-blocking antibody (Fig. 6A and B), a decrease in insulin and IGF1 receptor phosphorylation (Fig. 6C and Supplementary Fig. S11), and a strong increase in cleaved caspase-3 levels in tumors cotreated with gemcitabine and IGF-blocking antibody (Fig. 6C). Combination of 5-FU or paclitaxel with BI 836845 only produced a slight decrease in tumor growth in this model (Supplementary Fig. S12A and S12B), despite an increase in tumor cell death (Supplementary Fig. S12C and S12D).

Taken together, these findings indicate that functional blockade of IGFs significantly increases the response of pancreatic tumors to gemcitabine *in vivo*.

Discussion

The data presented herein describe that stromal-derived IGFs are a critical inducer of chemoresistance in pancreatic cancer, and provide preclinical data that support the rationale for using IGF-blocking antibodies in combination with gemcitabine for the treatment of pancreatic cancer (Fig. 6D). In these studies, we report a direct role for TAMs and myofibroblasts in chemoresistance of pancreatic cancer cells, and a paracrine signaling loop in which stromal-derived IGFs activate the insulin/IGF1R survival signaling pathway and blunt response of pancreatic cancer cells to chemotherapy. A recent study describes how fibroblasts exposed to pancreatic cancer cells secrete IGF, and this leads to pancreatic cancer cell survival and proliferation *in vitro* (44). In agreement with these findings, in this study, we further confirm that production of IGF by stromal cells occurs in pancreatic tumors *in vivo* and that both macrophages and myofibroblasts are the two major sources of IGFs within the pancreatic tumor microenvironment. In addition, we found that in humans, the

insulin/IGF1R signaling pathway is activated in 38 of 53 (~72%) of PDAC patient samples, and this strongly positively correlates with an increase in $CD163^+$ (M2-like) TAMs.

On the basis of these findings, we explored the therapeutic opportunities of combining gemcitabine with IGF inhibition in preclinical models of pancreatic cancer, and found that indeed, inhibition of IGFs signaling increases response of pancreatic tumors to gemcitabine.

While IGF receptor inhibitors failed in the clinics (41, 45–47), two IGF-blocking antibodies, MEDI-573 and BI 836845, are being evaluated in phase II clinical trials for metastatic breast cancer (MEDI-573), and metastatic breast cancer and castration-resistant prostate cancer (BI 836845; Clinicaltrials.gov Identifiers: NCT02204072, NCT01446159, NCT02123823). In contrast to IGF1 receptor inhibitors, which only inhibit signaling through IGF1 receptor, IGF ligand–blocking antibodies inhibit proliferative (but not metabolic) signaling through both IGF1 and insulin receptors. The studies described here provide the proof-of-principle for further evaluation of IGF-blocking antibodies in combination with gemcitabine for the treatment of patients with pancreatic cancer.

Despite extensive efforts invested in the clinical development of therapies against PDAC, current standard treatments only exert a modest effect, and targeting only the tumor cells has not resulted in a significant improvement in patient outcome (30, 31). The rich stromal compartment present in PDAC is not inert, and instead provides a variety of nonmalignant stromal cells and extracellular matrix proteins, which support tumor initiation, progression, and drug resistance (11, 20, 22, 23, 32, 35, 41, 42). Thus, therapies that target both the neoplastic cells and the protumorigenic functions of the stromal compartment will likely achieve a better therapeutic response.

TAMs can enhance or limit the efficacy of chemotherapy depending on the tumor model, the tumor stage and/or the chemotherapeutic agent used. For example, chemoresistance is increased when cytotoxic agents increase M2-like macrophage infiltration via CCL2 (48) or CSF1 (21). Macrophages can also impair host responses to chemotherapy by expressing cathepsins that activate chemoprotective T cells (18, 19) or by inducing the upregulation of cytidine deaminase, an enzyme that metabolizes nucleoside analogues (20). TAMs demonstrate a high degree of plasticity, and can be polarized into M1-like antitumorigenic and M2-like protumorigenic macrophages (49). Previous studies targeting signaling pathways necessary for the recruitment of macrophages or specific chemotactic factors (CCL2/PI3Kγ/CSF1) have provided proof-of-concept that macrophages represent an attractive target to reduce tumor progression (13, 14, 21, 22, 41, 50). However, dependent on the microenvironmental cytokine milieu, macrophages are not only promoting tumor growth, but they can also critically orchestrate an antitumor immune response (9). Thus, therapies that aim to specifically inhibit the protumorigenic functions of macrophages, while sparing their tumoricidal activity, could act as an alternative, and perhaps, more efficient approach than therapies that completely block macrophage recruitment to the tumor (27, 28). In this regard, our studies indicate that IGF blockade increases pancreatic tumors' response to gemcitabine without affecting immune cell infiltration, including macrophage infiltration, or without affecting macrophage polarization. Interestingly, a recent elegant study also

describes macrophage-derived IGF as a key driver of resistance to CSF-1R inhibition in glioblastoma (51).

In conclusion, our studies suggest that in PDAC, stroma-derived IGFs can blunt the response to chemotherapy via an IGF-insulin/IGF1R paracrine signaling axis, and provide the rationale for further evaluating the combination of gemcitabine with IGF signaling blockade in pancreatic cancer treatment.

Supplementary Material

Refer to Web version on PubMed Central for supplementary material.

Acknowledgments

We thank Professors R. O'Connor, G. Cohen, M. Clague, S. Urbe, and D. Palmer for discussions and sharing reagents and protocols. We thank A. Linford for technical help with immunohistochemistry and N. Bird for collecting blood from healthy volunteers. We thank Boehringer Ingelheim for providing us with the IGF-blocking antibody BI 836845. We also acknowledge the Liverpool Tissue Bank for providing tissue samples, and the Liverpool Centre for Cell Imaging (CCI), the flow cytometry/cell sorting facility, and the biomedical science unit for provision of equipment and technical assistance. We thank the patients and their families, as well as the healthy blood donors who contributed with tissue samples and blood donations to these studies.

Grant Support

These studies were supported by a Sir Henry Dale research fellowship to A. Mielgo, jointly funded by the Wellcome Trust and the Royal Society (grant number 102521/Z/13/Z), a New Investigator research grant from the Medical Research Council to M.C. Schmid (grant number MR/L000512/1) and North West Cancer Research funding to A. Mielgo and M.C. Schmid.

The costs of publication of this article were defrayed in part by the payment of page charges. This article must therefore be hereby marked *advertisement* in accordance with 18 U.S.C. Section 1734 solely to indicate this fact.

References

1. Holohan C, Van Schaeybroeck S, Longley DB, Johnston PG. Cancer drug resistance: an evolving paradigm. Nat Rev Cancer. 2013; 13:714–26. [PubMed: 24060863]
2. McMillin DW, Negri JM, Mitsiades CS. The role of tumour-stromal interactions in modifying drug response: challenges and opportunities. Nat Rev Drug Discov. 2013; 12:217–28. [PubMed: 23449307]
3. Klemm F, Joyce JA. Microenvironmental regulation of therapeutic response in cancer. Trends Cell Biol. 2015; 25:198–213. [PubMed: 25540894]
4. Mielgo A, Seguin L, Huang M, Camargo MF, Anand S, Franovic A, et al. A MEK-independent role for CRAF in mitosis and tumor progression. Nat Med. 2011; 17:1641–5. [PubMed: 22081024]
5. Seguin L, Kato S, Franovic A, Camargo MF, Lesperance J, Elliott KC, et al. An integrin β3-KRAS-RalB complex drives tumour stemness and resistance to EGFR inhibition. Nat Cell Biol. 2014; 16:457–68. [PubMed: 24747441]
6. Advani SJ, Camargo MF, Seguin L, Mielgo A, Anand S, Hicks AM, et al. Kinase-independent role for CRAF-driving tumour radioresistance via CHK2. Nat Commun. 2015; 3:8154.
7. Noy R, Pollard JW. Tumor-associated macrophages: from mechanisms to therapy. Immunity. 2014; 41:49–61. [PubMed: 25035953]
8. Mantovani A, Allavena P. The interaction of anticancer therapies with tumor-associated macrophages. J Exp Med. 2015; 212:435–45. [PubMed: 25753580]
9. De Palma M, Lewis CE. Macrophage regulation of tumor responses to anticancer therapies. Cancer Cell. 2013; 23:277–86. [PubMed: 23518347]

Europe PMC Funders Author Manuscripts

10. Junttila MR, de Sauvage FJ. Influence of tumour micro-environment heterogeneity on therapeutic response. Nature. 2013; 501:346–54. [PubMed: 24048067]
11. Liou GY, Doppler H, Necela B, Edenfield B, Zhang L, Dawson DW, et al. Mutant KRAS-induced expression of ICAM-1 in pancreatic acinar cells causes attraction of macrophages to expedite the formation of precancerous lesions. Cancer Discov. 2015; 5:52–63. [PubMed: 25361845]
12. Lin EY, Nguyen AV, Russell RG, Pollard JW. Colony-stimulating factor 1 promotes progression of mammary tumors to malignancy. J Exp Med. 2001; 193:727–40. [PubMed: 11257139]
13. Qian BZ, Li J, Zhang H, Kitamura T, Zhang J, Campion LR, et al. CCL2 recruits inflammatory monocytes to facilitate breast-tumour metastasis. Nature. 2011; 475:222–5. [PubMed: 21654748]
14. Qian BZ, Zhang H, Li J, He T, Yeo EJ, Soong DY, et al. FLT1 signaling in metastasis-associated macrophages activates an inflammatory signature that promotes breast cancer metastasis. J Exp Med. 2015; 212:1433–48. [PubMed: 26261265]
15. Schmid MC, Avraamides CJ, Dippold HC, Franco I, Foubert P, Ellies LG, et al. Receptor tyrosine kinases and TLR/IL1Rs unexpectedly activate myeloid cell PI3kgamma, a single convergent point promoting tumor inflammation and progression. Cancer Cell. 2011; 19:715–27. [PubMed: 21665146]
16. Schmid MC, Avraamides CJ, Foubert P, Shaked Y, Kang SW, Kerbel RS, et al. Combined blockade of integrin-alpha4beta1 plus cytokines SDF-1alpha or IL-1beta potently inhibits tumor inflammation and growth. Cancer Res. 2011; 71:6965–75. [PubMed: 21948958]
17. Schmid MC, Franco I, Kang SW, Hirsch E, Quilliam LA, Varner JA. PI3-kinase gamma promotes Rap1a-mediated activation of myeloid cell integrin alpha4beta1, leading to tumor inflammation and growth. PLoS One. 2013; 8:e60226. [PubMed: 23565202]
18. Shree T, Olson OC, Elie BT, Kester JC, Garfall AL, Simpson K, et al. Macrophages and cathepsin proteases blunt chemotherapeutic response in breast cancer. Genes Dev. 2011; 25:2465–79. [PubMed: 22156207]
19. Bruchard M, Mignot G, Derangere V, Chalmin F, Chevriaux A, Vegran F, et al. Chemotherapy-triggered cathepsin B release in myeloid-derived suppressor cells activates the Nlrp3 inflammasome and promotes tumor growth. Nat Med. 2013; 19:57–64. [PubMed: 23202296]
20. Weizman N, Krelin Y, Shabtay-Orbach A, Amit M, Binenbaum Y, Wong RJ, et al. Macrophages mediate gemcitabine resistance of pancreatic adenocarcinoma by upregulating cytidine deaminase. Oncogene. 2014; 33:3812–9. [PubMed: 23995783]
21. DeNardo DG, Brennan DJ, Rexhepaj E, Ruffell B, Shiao SL, Madden SF, et al. Leukocyte complexity predicts breast cancer survival and functionally regulates response to chemotherapy. Cancer Discov. 2011; 1:54–67. [PubMed: 22039576]
22. Mitchem JB, Brennan DJ, Knolhoff BL, Belt BA, Zhu Y, Sanford DE, et al. Targeting tumor-infiltrating macrophages decreases tumor-initiating cells, relieves immunosuppression, and improves chemotherapeutic responses. Cancer Res. 2013; 73:1128–41. [PubMed: 23221383]
23. Nielsen SR, Quaranta V, Linford A, Emeagi P, Rainer C, Santos A, et al. Macrophage-secreted granulin supports pancreatic cancer metastasis by inducing liver fibrosis. Nat Cell Biol. 2016; 18:549–60. [PubMed: 27088855]
24. Murray PJ, Wynn TA. Protective and pathogenic functions of macrophage subsets. Nat Rev Immunol. 2011; 11:723–37. [PubMed: 21997792]
25. Ruffell B, Affara NI, Coussens LM. Differential macrophage programming in the tumor microenvironment. Trends Immunol. 2012; 33:119–26. [PubMed: 22277903]
26. Sica A, Mantovani A. Macrophage plasticity and polarization: in vivo veritas. J Clin Invest. 2012; 122:787–95. [PubMed: 22378047]
27. Quail DF, Joyce JA. Microenvironmental regulation of tumor progression and metastasis. Nat Med. 2013; 19:1423–37. [PubMed: 24202395]
28. Bronte V, Murray PJ. Understanding local macrophage phenotypes in disease: modulating macrophage function to treat cancer. Nat Med. 2015; 21:117–9. [PubMed: 25654601]
29. Conroy T, Desseigne F, Ychou M, Bouche O, Guimbaud R, Becouarn Y, et al. FOLFIRINOX versus gemcitabine for metastatic pancreatic cancer. N Engl J Med. 2011; 364:1817–25. [PubMed: 21561347]

30. Von Hoff DD, Ramanathan RK, Borad MJ, Laheru DA, Smith LS, Wood TE, et al. Gemcitabine plus nab-paclitaxel is an active regimen in patients with advanced pancreatic cancer: a phase I/II trial. J Clin Oncol. 2011; 29:4548–54. [PubMed: 21969517]
31. Shibuya KC, Goel VK, Xiong W, Sham JG, Pollack SM, Leahy AM, et al. Pancreatic ductal adenocarcinoma contains an effector and regulatory immune cell infiltrate that is altered by multimodal neoadjuvant treatment. PLoS One. 2014; 9:e96565. [PubMed: 24794217]
32. Gunderson AJ, Kaneda MM, Tsujikawa T, Nguyen AV, Affara NI, Ruffell B, et al. Bruton's Tyrosine Kinase (BTK)-dependent immune cell crosstalk drives pancreas cancer. Cancer Discov. 2015; 6:270–85. [PubMed: 26715645]
33. Feig C, Gopinathan A, Neesse A, Chan DS, Cook N, Tuveson DA. The pancreas cancer microenvironment. Clin Cancer Res. 2012; 18:4266–76. [PubMed: 22896693]
34. Hingorani SR, Wang L, Multani AS, Combs C, Deramaudt TB, Hruban RH, et al. Trp53R172H and KrasG12D cooperate to promote chromosomal instability and widely metastatic pancreatic ductal adenocarcinoma in mice. Cancer cell. 2005; 7:469–83. [PubMed: 15894267]
35. Olive KP, Jacobetz MA, Davidson CJ, Gopinathan A, McIntyre D, Honess D, et al. Inhibition of Hedgehog signaling enhances delivery of chemotherapy in a mouse model of pancreatic cancer. Science. 2009; 324:1457–61. [PubMed: 19460966]
36. Friedbichler K, Hofmann MH, Kroez M, Ostermann E, Lamche HR, Koessl C, et al. Pharmacodynamic and antineoplastic activity of BI 836845, a fully human IGF ligand-neutralizing antibody, and mechanistic rationale for combination with rapamycin. Mol Cancer Ther. 2014; 13:399–409. [PubMed: 24296829]
37. Schmittgen TD, Livak KJ. Analyzing real-time PCR data by the comparative C(T) method. Nat Protoc. 2008; 3:1101–8. [PubMed: 18546601]
38. Lawrence T, Natoli G. Transcriptional regulation of macrophage polarization: enabling diversity with identity. Nat Rev Immunol. 2011; 11:750–61. [PubMed: 22025054]
39. Denduluri SK, Idowu O, Wang Z, Liao Z, Yan Z, Mohammed MK, et al. Insulin-like growth factor (IGF) signaling in tumorigenesis and the development of cancer drug resistance. Genes Dis. 2015; 2:13–25. [PubMed: 25984556]
40. Pollak M. The insulin and insulin-like growth factor receptor family in neoplasia: an update. Nat Rev Cancer. 2012; 12:159–69. [PubMed: 22337149]
41. Zhu Y, Knolhoff BL, Meyer MA, Nywening TM, West BL, Luo J, et al. CSF1/CSF1R blockade reprograms tumor-infiltrating macrophages and improves response to T-cell checkpoint immunotherapy in pancreatic cancer models. Cancer Res. 2014; 74:5057–69. [PubMed: 25082815]
42. Pylayeva-Gupta Y, Das S, Handler JS, Hajdu CH, Coffre M, Koralov S, et al. IL-35 producing B cells promote the development of pancreatic neoplasia. Cancer Discov. 2015; 6:247–55. [PubMed: 26715643]
43. Torres MP, Rachagani S, Souchek JJ, Mallya K, Johansson SL, Batra SK. Novel pancreatic cancer cell lines derived from genetically engineered mouse models of spontaneous pancreatic adenocarcinoma: applications in diagnosis and therapy. PLoS One. 2013; 8:e80580. [PubMed: 24278292]
44. Tape CJ, Ling S, Dimitriadi M, McMahin KM, Worboys JD, Leong HS, et al. Oncogenic KRAS regulates tumor cell signaling via stromal reciprocation. Cell. 2016; 165:910–20. [PubMed: 27087446]
45. Guha M. Anticancer IGF1R classes take more knocks. Nat Rev Drug Discov. 2013; 12:250. [PubMed: 23535923]
46. King H, Aleksic T, Haluska P, Macaulay VM. Can we unlock the potential of IGF-1R inhibition in cancer therapy? Cancer Treat Rev. 2014; 40:1096–05. [PubMed: 25123819]
47. Gradishar WJ, Yardley DA, Layman R, Sparano JA, Chuang E, Northfelt DW, et al. Clinical and translational results of a phase II, randomized trial of an anti-IGF-1R (Cixutumumab) in women with breast cancer that progressed on endocrine therapy. Clin Cancer Res. 2016; 22:301–9. [PubMed: 26324738]

48. Nakasone ES, Askautrud HA, Kees T, Park JH, Plaks V, Ewald AJ, et al. Imaging tumor-stroma interactions during chemotherapy reveals contributions of the microenvironment to resistance. Cancer Cell. 2012; 21:488–503. [PubMed: 22516258]

49. Mills CD, Lenz LL, Harris RA. A breakthrough: macrophage-directed cancer immunotherapy. Cancer Res. 2016; 76:513–6. [PubMed: 26772756]

50. Pyonteck SM, Akkari L, Schuhmacher AJ, Bowman RL, Sevenich L, Quail DF, et al. CSF-1R inhibition alters macrophage polarization and blocks glioma progression. Nat Med. 2013; 19:1264–72. [PubMed: 24056773]

51. Quail DF, Bowman RL, Akkari L, Quick ML, Schuhmacher AJ, Huse JT, et al. The tumor microenvironment underlies acquired resistance to CSF-1R inhibition in gliomas. Science. 2016; 352:aad3018. [PubMed: 27199435]

Europe PMC Funders Author Manuscripts

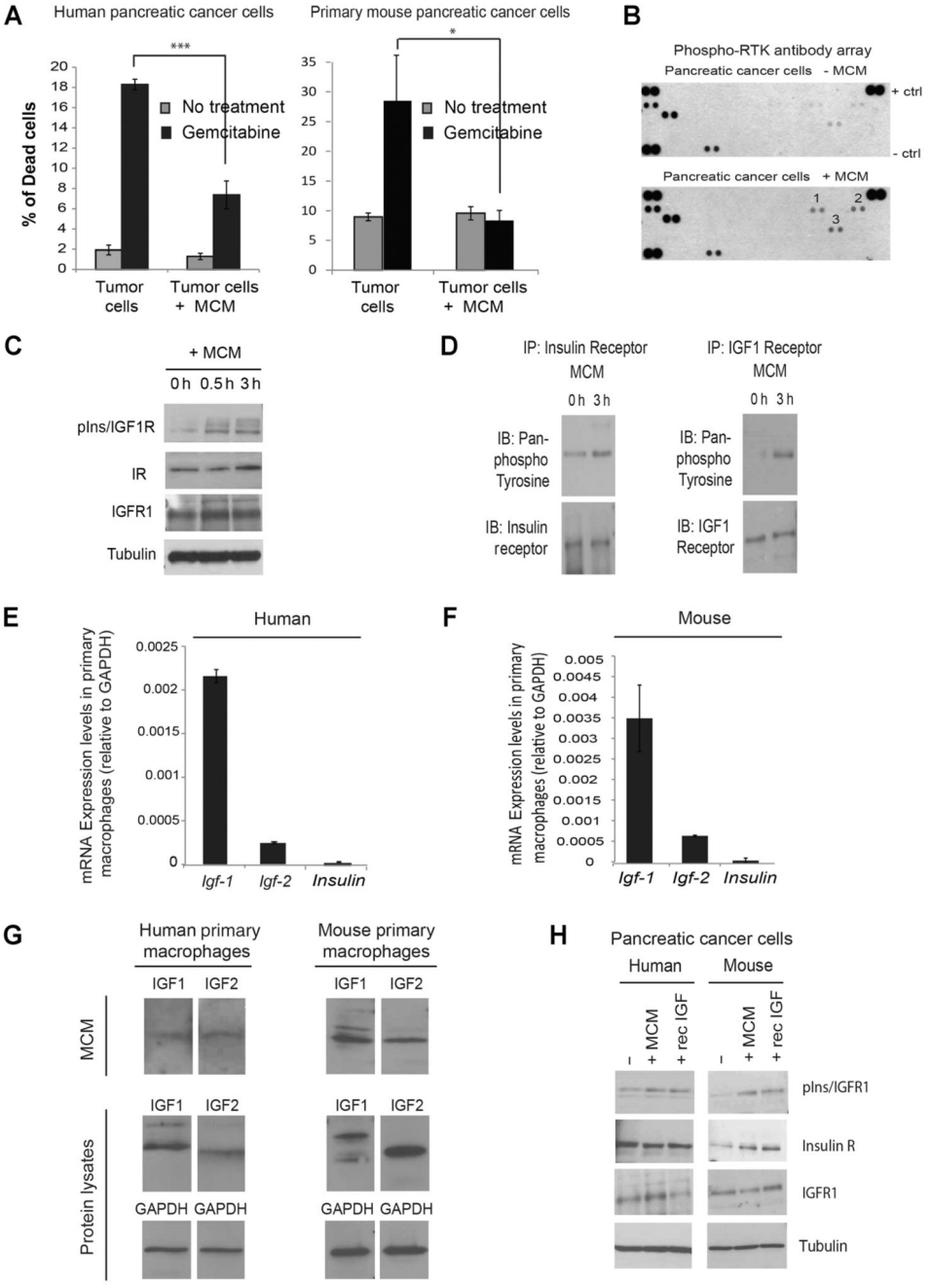

Figure 1. Macrophage-secreted factors directly induce chemoresistance and activate insulin/IGF1 receptors in pancreatic cancer cells.

A, Left, human pancreatic SUIT-2 cancer cells were cultured in the presence or absence of MCM from human primary macrophages and treated with 200 nmol/L gemcitabine for 24 hours or left untreated. Percentage of cell death was quantified by flow cytometry. Error bars, SD. ($n = 4$); two-tailed unpaired t test; ***, $P \leq 0.005$. Right, mouse primary KPC-derived pancreatic cancer cells were cultured in the presence or absence of MCM from mouse primary macrophages and treated with 200 nmol/L gemcitabine for 24 hours or left untreated. Percentage of cell death was quantified by flow cytometry. Error bars, SD ($n = 3$);

Europe PMC Funders Author Manuscripts

two-tailed unpaired *t* test; *, $P \leq 0.05$. **B**, Human pancreatic cancer SUIT-2 cells were serum starved for 24 hours and exposed for 2 hours to human MCM, or left unexposed, and protein lysates were subjected to a phospho-receptor tyrosine kinase array. 1, phospho-insulin receptor; 2, phospho-AXL receptor; 3, phospho-Ephrin receptor. **C**, Immunoblotting analysis of phospho-insulin/IGF1 receptors, insulin receptor, IGF1 receptor, and tubulin in SUIT-2 cells serum starved or exposed to MCM for 30 minutes or 3 hours. **D**, Immunoblotting analysis of pan-phospho tyrosine, insulin receptor, and IGFR1 in insulin and IGFR1 immunoprecipitates of SUIT-2 cells treated with human MCM for 3 hours or left untreated. **E**, Quantification of *Igf1, Igf2,* and *Insulin* mRNA expression levels in human primary macrophages ($n = 3$). **F**, Quantification of *Igf1, Igf2*, and *Insulin* mRNA expression levels in mouse primary macrophages ($n = 3$). **G**, Immunoblotting analysis of IGF1 and IGF2 ligands in human and mouse MCM and macrophage lysates. **H**, Immunoblotting analysis of phospho-insulin/IGF1 receptor, insulin receptor, IGFR1 and tubulin, in human pancreatic cancer SUIT-2 cells, and murine primary KPC-derived pancreatic cancer cells serum starved, exposed to MCM, or exposed to recombinant IGF for 3 hours.

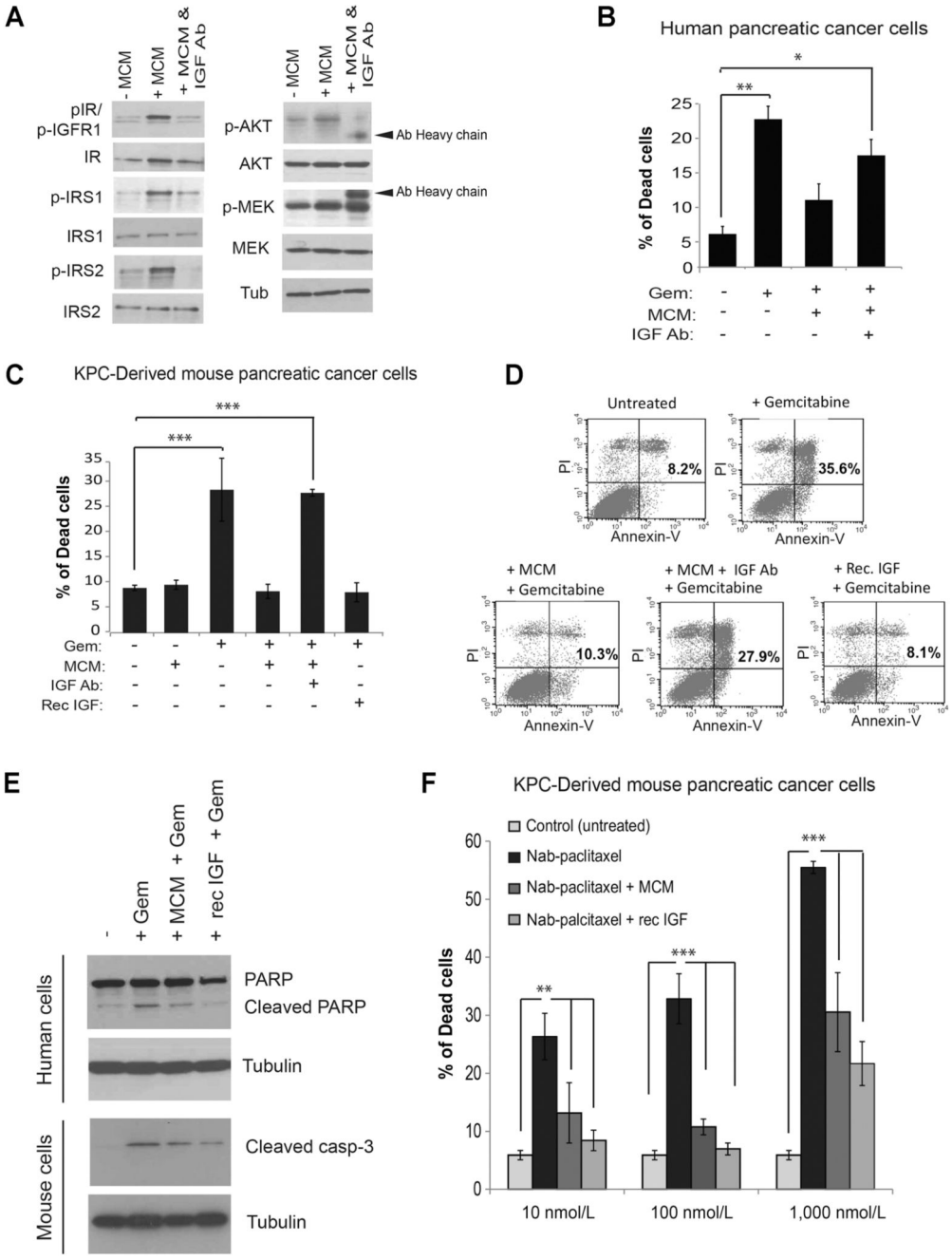

Figure 2. Blockade of IGF impairs macrophage-mediated chemoresistance of pancreatic cancer cells.

A, Immunoblotting analysis of SUIT-2 cells untreated or treated with MCM or MCM+IGF-blocking antibody for 3 hours. **B**, Quantification of cell death in SUIT-2 cells treated with gemcitabine, MCM, and IGF-blocking antibody for 24 hours. Error bars, SD. ($n = 3$); **, $P \leq 0.01$; *, $P \leq 0.05$ using one-way ANOVA and Tukey *post hoc* test. **C**, Quantification of cell death in primary mouse KPC-derived pancreatic cancer cells untreated or treated with gemcitabine, MCM, IGF-blocking antibody, or recombinant IGF for 24 hours. Error bars,

Europe PMC Funders Author Manuscripts

SD. ($n = 3$); ***, $P \leq 0.005$ using one-way ANOVA and Tukey *post hoc* test. **D**, Representative flow cytometry dot blots of KPC-derived cells exposed to gemcitabine, MCM, IGF-blocking antibody, and recombinant IGF. **E**, Immunoblotting analysis of PARP and tubulin in human SUIT-2 pancreatic cancer cells and cleaved caspase-3 and tubulin in KPC-derived mouse pancreatic cancer cells untreated, treated with gemcitabine, MCM + gemcitabine, or recombinant IGF + gemcitabine for 24 hours. **F**, Quantification of cell death in KPC-derived cells cultured in the presence or absence of MCM or recombinant IGF and treated with 10, 100, or 1,000 nmol/L nab-paclitaxel for 36 hours. Error bars, SD ($n = 3$); ***, $P \leq 0.005$; **, $P \leq 0.01$ using one-way ANOVA and Tukey *post hoc* test.

Europe PMC Funders Author Manuscripts

Europe PMC Funders Author Manuscripts

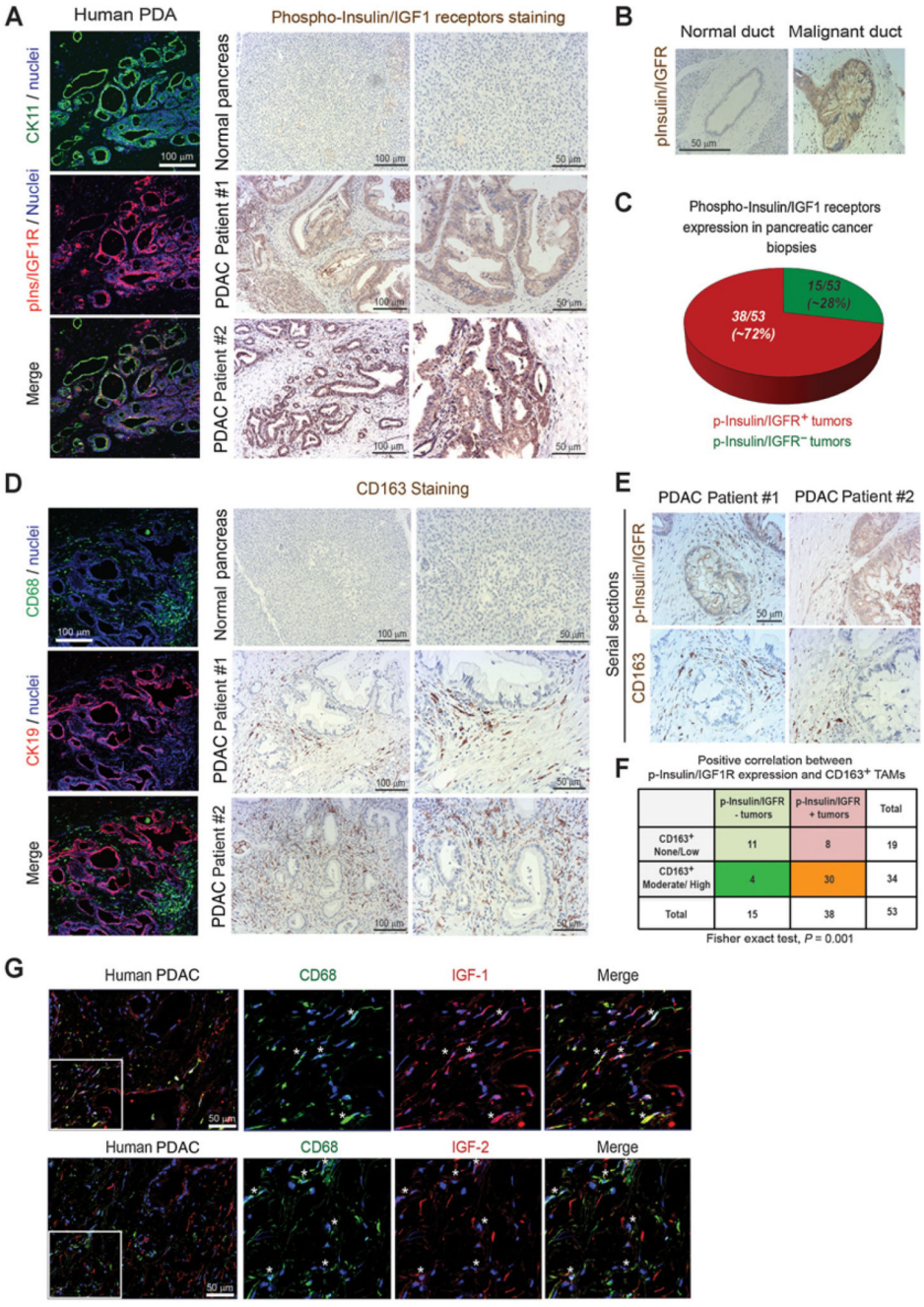

Figure 3. Insulin and IGF1 receptors are activated on cancer cells in biopsies from patients with PDAC, and this correlates with increased numbers of TAMs.

A, Left, confocal microscopy images of frozen human PDAC tissues immunofluorescently costained for the tumor epithelial marker CK11 (green), phospho-insulin/IGF1 receptors (red), and nuclei (blue). Scale bar, 100 μm. Right, immunohistochemical staining of phospho-insulin/IGF1 receptors in normal human pancreas and biopsies from patients with PDAC. Scale bars, 100 μm and 50 μm. **B**, Images of normal and malignant human pancreatic ducts immunohistochemically stained for phospho-insulin/IGF1 receptors. Scale bar, 50 μm.

C, Pie diagram representing the percentage of phospho-insulin/IGF1 receptor–positive (red) and negative (green) tumors assessed in tissue microarrays containing biopsies from 53 consented PDAC patients. **D**, Left, confocal microscopy images of frozen human PDAC tissues immunofluorescently costained for CD68 (green), CK19 (red), and nuclei (blue). Scale bar, 100 μm. Right, immunohistochemical staining of CD163 in normal human pancreas and biopsies from patients with PDAC. Scale bars, 100 μm and 50 μm. **E**, Serial sections of biopsies from human PDAC samples immunohistochemically stained for phospho-insulin/IGF1 receptors and CD163. Scale bar, 50 μm. **F**, Contingency table and results from statistical analysis showing a strong evidence of positive correlation between phospho-insulin/IGF1R expression in tumors and increased $CD163^+$ macrophage infiltration. Relative risk = 4.92 [95% confidence interval (CI), 1.82–13.34], $P = 0.001$ using Fisher exact test. **G**, Immunofluorescent images of human PDAC tissues stained for CD68 (green), IGF1 or IGF2 (red) and nuclei (blue). White stars, $CD68^+$ macrophages that express IGF1 or IGF2. Scale bar, 50 μm.

Europe PMC Funders Author Manuscripts

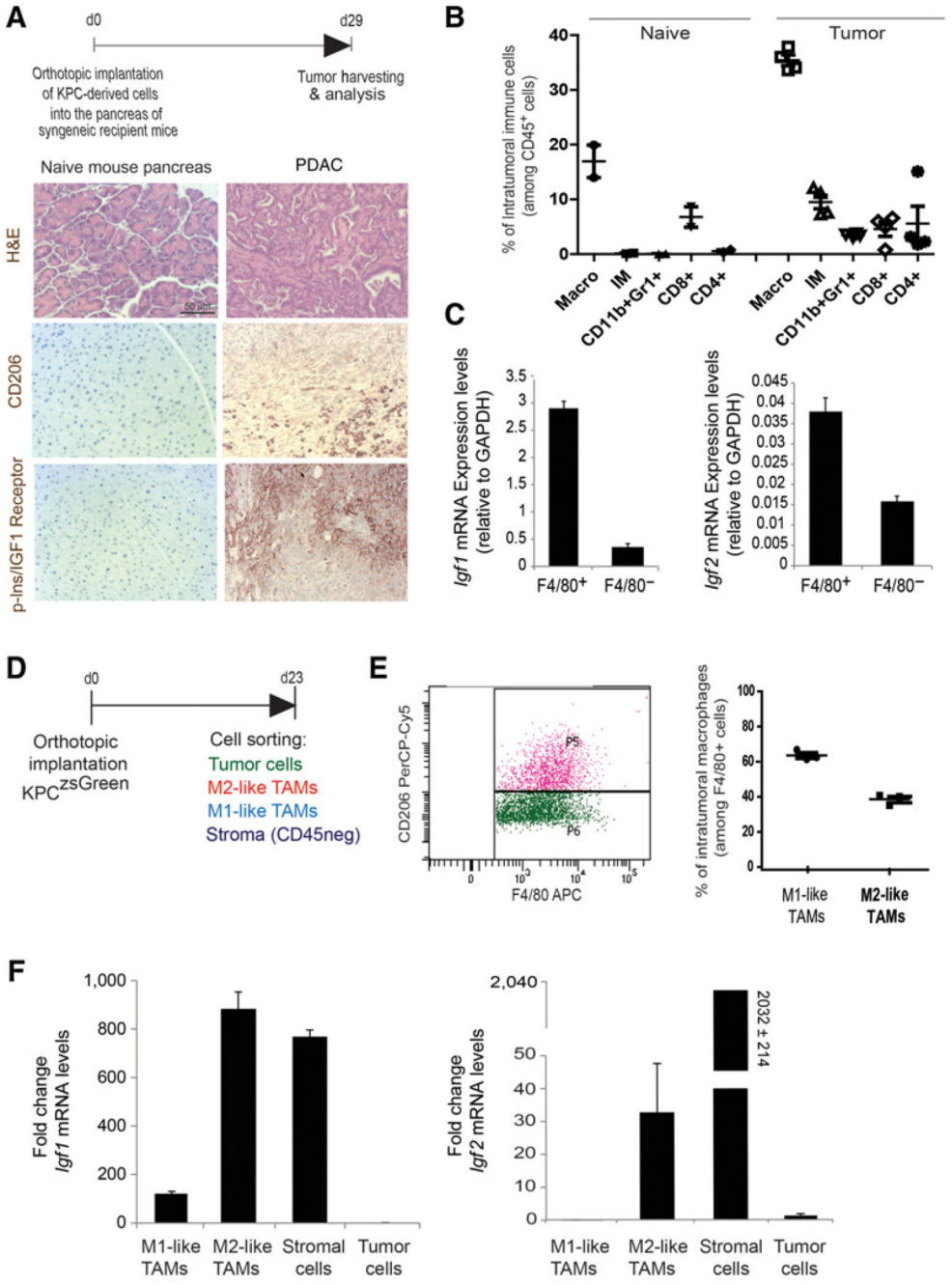

Figure 4. TAMs and myofibroblasts are major sources of IGF1 and IGF2 in pancreatic tumors.

A, KPC-derived tumor cells were orthotopically implanted into the pancreas of syngeneic recipient mice. Images show H&E, CD206, and phospho-insulin/IGF1 receptors staining of naïve mouse pancreas and murine PDAC tissue samples harvested 29 days after tumor implantation. **B**, Normal pancreas from naïve mice and pancreatic tumors were harvested and digested on day 29 after implantation. Percentage of intratumoral F4/80^{+} macrophages, Gr1^{+}/CD11b^{+} neutrophils and myeloid-derived suppressor cells, CD4^{+} and CD8^{+} T cells, among CD45^{+} immune cells, were quantified by flow cytometry (n = 2 normal pancreas; n =

4 pancreatic carcinomas). **C**, Quantification of *Igf1* and *Igf2* mRNA expression levels in F4/80^{+} and F4/80^{-} cells isolated from pancreatic tumors. Error bars, SD (n = 3). **D**, KPC$^{luc/zsGreen}$ (zsGreen)-derived tumor cells (FC1242$^{luc/zsGreen}$) were orthotopically implanted into the pancreas of syngeneic recipient (C57/BL6) mice. Tumors were harvested and digested at day 23 after implantation and tumor cells, nonimmune stromal cells, M1-like and M2-like macrophages were sorted by flow cytometry. **E**, Dot blot showing F4/80^{+}/CD206^{+} and F4/80^{+}/CD206^{-} intratumoral macrophages (left) and the percentage of F4/80^{+}/CD206^{-}M1-like macrophages and F4/80^{+}/CD206^{+} M2-like macrophages in pancreatic tumors (right). **F**, Quantification of *Igf1* (left) and *Igf2* (right) mRNA expression levels in CD45^{+}/F4/80^{+}/CD206^{-} M1-like macrophages, CD45^{+}/F4/80^{+}/CD206^{+} M2-like macrophages, CD45^{-}/zsGreen^{-} nonimmune stromal cells, and CD45^{-}/zsGreen^{+} tumor cells isolated from murine pancreatic tumors. Error bars, SD (n = 3).

Europe PMC Funders Author Manuscripts

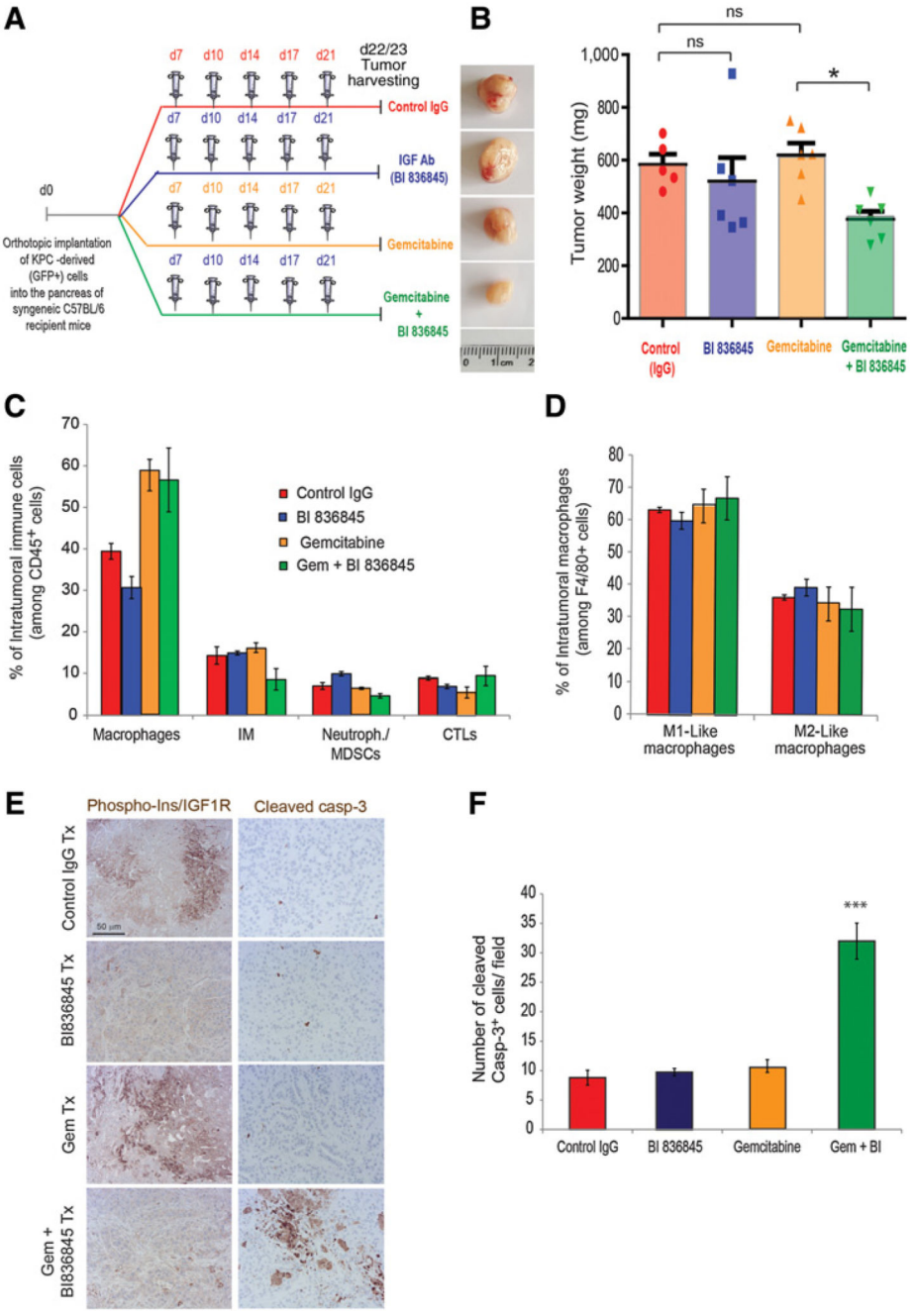

Figure 5. Combination of gemcitabine with IGF-blocking antibody BI 836845 inhibits tumor growth in a syngeneic orthotopic pancreatic cancer model.

A, KPC$^{luc/zsGreen}$ (zsGreen)-derived pancreatic tumor cells (FC1242$^{luc/zsGreen}$) were orthotopically implanted into the pancreas of syngeneic C57BL/6 recipient mice, and mice were treated, starting at day 7 after tumor implantation, twice a week intraperitoneally with either control IgG antibody, gemcitabine (100 mg/kg), IGF-blocking antibody BI 836845 (100 mg/kg), or a combination of gemcitabine with BI 836845. **B**, Representative images of tumors and tumor weights are shown ($n = 6$ mice per group); *, $P \leq 0.05$ using one-way

ANOVA and Tukey *post hoc* test. **C**, Pancreatic tumors were digested and percentage of intratumoral F4/80$^+$ macrophages, Ly6C$^+$/Ly6G$^-$ inflammatory monoctyes, Gr1$^+$/CD11b$^+$ neutrophils and myeloid-derived suppressor cells (MDSC), and CD8$^+$ cytotoxic T cells (CTL), among CD45$^+$ immune cells, were quantified by flow cytometry. **D**, Percentage of intratumoral CD206$^-$ M1-like macrophages and CD206$^+$ M2-like macrophages, among F4/80$^+$ macrophages, were quantified by flow cytometry. **E**, Immunohistochemical staining of phospho-insulin/IGF1R and cleaved caspase-3 in pancreatic tumors treated with IgG (control), gemcitabine, IGF-blocking antibody BI 836845, or gemcitabine + BI 836845. **F**, Quantification of cleaved caspase-3–positive dead cells in tumors treated with IgG (control), gemcitabine, IGF-blocking antibody BI 836845, or gemcitabine + BI 836845 (8–11 fields counted/mouse tumor); ***, $P \leq 0.005$ compared with other treatment groups, using one-way ANOVA and Tukey *post hoc* test.

Europe PMC Funders Author Manuscripts

Europe PMC Funders Author Manuscripts

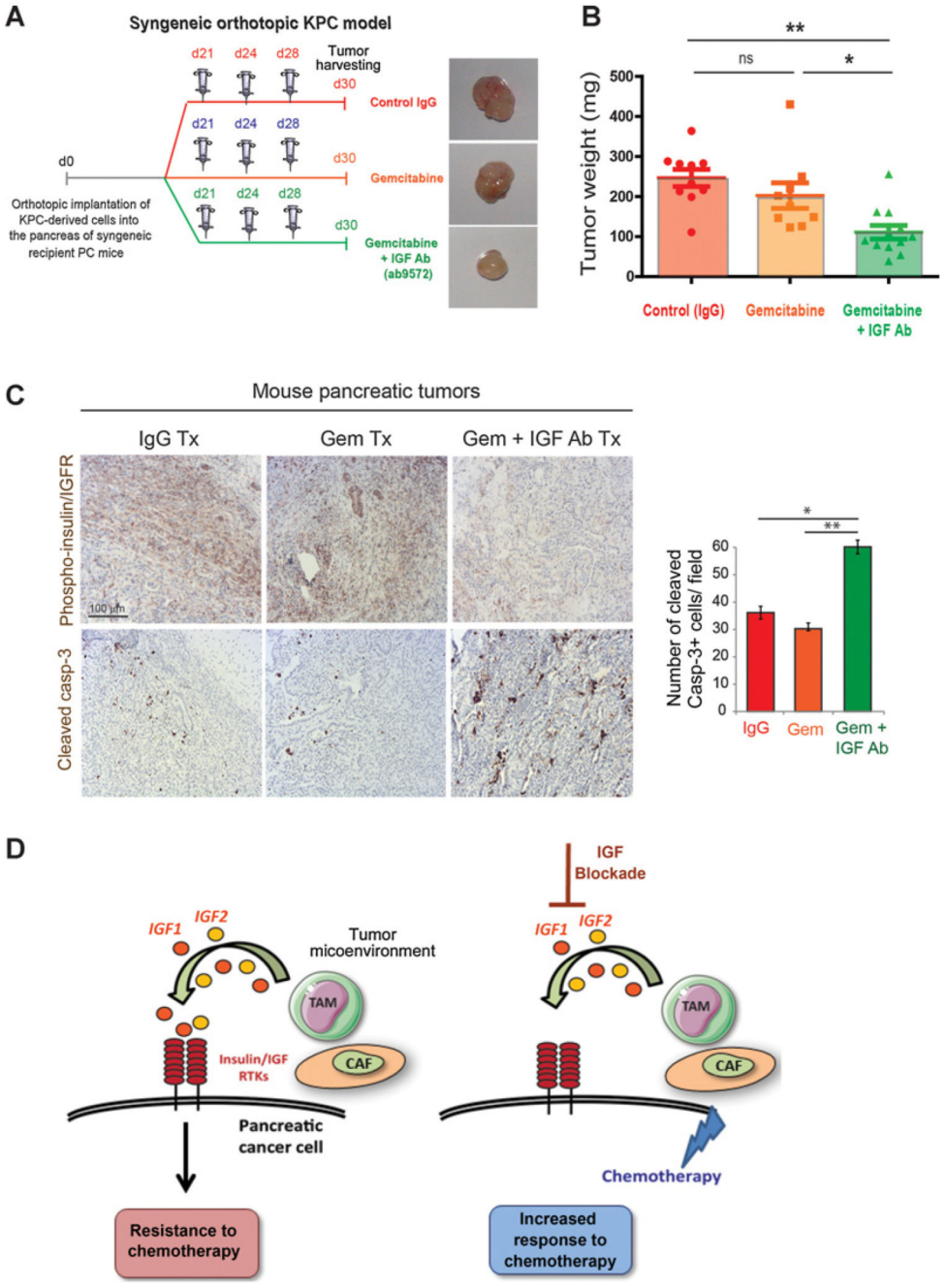

Figure 6. Combination of gemcitabine with IGF-blocking antibody ab9572 decreases tumor growth in a syngeneic orthotopic pancreatic cancer model.

A, Primary mouse KPC-derived pancreatic cancer cells were implanted orthotopically in the pancreas of syngeneic recipient mice. Mice were administered intraperitoneally twice a week with IgG antibody, gemcitabine alone, or gemcitabine with an IGF-blocking antibody from Abcam (ab9572). Tumors were harvested at day 30 and representative images are shown. **B**, Tumor weights are shown (n = 9–12 mice per group). **, $P \leq 0.01$; *, $P \leq 0.05$ using one-way ANOVA and Tukey *post hoc* test. **C**, Left, immunohistochemical staining of

phospho-insulin/IGF1R, and cleaved caspase-3 in pancreatic tumors treated with IgG, gemcitabine, or gemcitabine + IGF-blocking antibody ab9572. Right, Quantification of cleaved caspase-3–positive dead cells in pancreatic tumors from mice treated with IgG control antibody, gemcitabine, or gemcitabine + ab9572 IGF-blocking antibody (6–8 fields counted/mouse tumor), **, $P \leq 0.01$ using one-way ANOVA and Tukey *post hoc* test. **D**, Schematics depicting the role of stroma-derived IGF in activation of the insulin/IGF1R signaling survival pathway and in mediating chemoresistance of pancreatic cancer cells.

Europe PMC Funders Author Manuscripts